ACTA MECHATRONICA

2020 Volume 5 Issue 3

International Scientific Journal about Mechatronics

electronic journal
ISSN 2453-7306

CONTENTS

(SEPTEMBER 2020)

(pages 35-40)
ANALYSIS OF INDUCTIVE SENSOR FIXING CLAMP IN RAILWAY APPLICATIONS
Barbara Schürger, Michal Kicko, Vojtech Neumann, Peter Frankovský

(pages 41-46)
COMPUTER SIMULATION USING MSC ADAMS
Darina Hroncová, Ingrid Delyová

Acta Mechatronica - International Scientific Journal about Mechatronics
Volume: 5 2020 Issue: 3 Pages: 35-40 ISSN 2453-7306

doi:10.22306/am.v5i3.66

Received: 30 June 2020
Revised: 25 July 2020
Accepted: 12 Aug. 2020

ANALYSIS OF INDUCTIVE SENSOR FIXING CLAMP IN RAILWAY APPLICATIONS

Barbara Schürger
Technical University of Košice, Faculty of Mechanical Engineering, Institute of Design Machine and Process Engineering, Department of Applied Mechanics and Mechanical Engineering, Letná 9, 042 00 Košice, Slovak Republic, EU, barbara.schurger@tuke.sk

Michal Kicko
Technical University of Košice, Faculty of Mechanical Engineering, Institute of Design Machine and Process Engineering, Department of Applied Mechanics and Mechanical Engineering, Letná 9, 042 00 Košice, Slovak Republic, EU, michal.kicko@tuke.sk

Vojtech Neumann
Technical University of Košice, Faculty of Mechanical Engineering, Institute of Design Machine and Process Engineering, Department of Applied Mechanics and Mechanical Engineering, Letná 9, 042 00 Košice, Slovak Republic, EU, Vojtech.Neumann@grob.de

Peter Frankovský
Technical University of Košice, Faculty of Mechanical Engineering, Institute of Design Machine and Process Engineering, Department of Applied Mechanics and Mechanical Engineering, Letná 9, 042 00 Košice, Slovak Republic, EU, peter.frankovsky@tuke.sk (corresponding author)

Keywords: static analysis, dynamic analysis, FEM, fixing clamp, railway application

Abstract: This paper provides static, modal and dynamic analysis of the assembly consisting of fixing clamp, inductive sensor, two fixing bolts and frame applied on railway stock. All the necessary tests to perform this analysis are in accordance with the standard EN 61373: 2010 or the Slovak standard STN EN 61373: 2011. In the next part, a simulation of the tests required for the dynamic analysis of the modelled assembly is performed. For each analysis, von Misses stress is evaluated and then compared to the yield strength of used material. Finally, this work provides a proposal for new design solutions of the fixing clamp based on the obtained results. All analyses were performed in ANSYS Workbench programme using finite element method.

1 Introduction

The rising standard of living increasing demands on the creation of optimal product design regarding the amount of time, money and material used. With the help of computer software, we can combine knowledge from several scientific disciplines, and thus create methods of solution and analysis in order to create the most optimal design solution [1]. Such solutions are particularly important in the areas of dynamic stress, to which the components on rolling stock are exposed as a result of their operation on railways. The force effect of dynamic loading varies in both magnitude and direction, and the nature of these changes affects how reliably the component will operate until the end of its expected life.

The aim of this paper was a dynamic analysis of the clamp fixing the OsiSense XS inductive proximity sensor from Telemecanique Sensors. This line of sensors provides functional and easy-to-install sensors that help to create much safer operation of the rolling stock.

2 Railway application

The sensors (Figure 1) with their fixing clamp applied to rolling stock are subjected to a deterministic harmonic load during operation as the railway wagon moves on smooth rails.

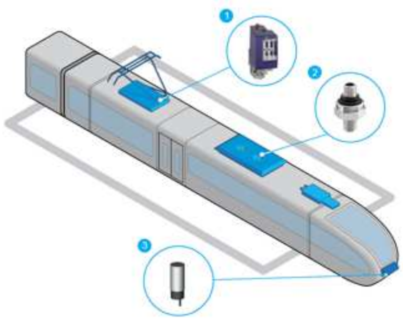

Figure 1 Types of sensor used in railway applications

For this reason, these parts must be subjected to the tests defined in standard EN 61373: 2011. This International Standard specifies requirements for the testing of components for use on railway vehicles that are subsequently exposed to vibration and shock due to the operating environment of the railway.

To ensure that the quality of the element is acceptable, it must withstand tests of a reasonably long time that simulate conditions throughout its expected life.

The test simulations were performed according to the procedures defined in the standard [2], specifically for two categories that were required in advance for fixing clamp analysis:

- **Category 1, Class B:** equipment mounted on the body of the rolling stock,
- **Category 2:** equipment mounted on the bogie of a rolling stock.

Table 1 Engineering data: Material properties

	Structural Steel 13 240	***Aluminium Alloy 6061***	***Plastic ABS***
Density ($kg.m^{-3}$)	7850	2770	1050
Young's Modulus (MPa)	$2{,}1.10^5$	$0{,}71.10^5$	$0{,}024.10^5$
Poisson's Ratio (-)	0,3	0,33	0,4078
Tensile Yield Strength (MPa)	250	164,8	36,13
Tensile Ultimate Strength (MPa)	460	246,1	38,73

Furthermore, it was necessary to define the individual excitation directions, namely:

- **Transverse direction:** in the direction of the X axis.
- **Longitudinal direction:** in the direction of the Y axis.
- **Vertical direction:** in the direction of the Z axis.

The aim of the research was to perform numerical simulations of random vibration tests and shock tests of a fixing clamp made of 3 different materials.

The basic model of fixing clamp is made of structural steel, while 2 other materials were designed during optimization, namely aluminium alloy 6061 (more expensive, but lighter than steel) and plastic Acrylonitrile-butadiene-styrene (cheaper and lighter than steel). Material properties of used materials are defined in Table 1.

3 Problem definition

The aim of the work was to perform numerical simulations of random vibration tests and impact tests, which are defined by the standard EN 61373: 2011 for equipment mounted on rail vehicles. In order to assess the quality of a component, it is necessary for the component to withstand, for a reasonable period, tests simulating the operation of the vehicle over its expected service life [3].

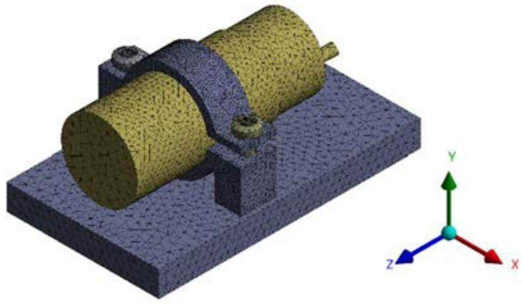

Figure 2 Analysed assembly

In the ANSYS Workbench program, a model of the fixing clamp with a sensor OsiSense XS, fixing bolts M5x40 and a frame was built. Then the model was discrete by quadratic hexagonal finite elements (Figure 2). Dimensions of the sensor and mounting bracket were given by the manufacturer.

4 Static analysis

After creating the finite element network, a static analysis was performed on the original structural steel. In the first step of the static calculation the fixed support and the bolt pretension was defined by calculating axial forces (1) based on the formula [4]:

$$F = \frac{M}{k.d} = \frac{2{,}68}{0{,}2.5.10^{-3}} = 2680\ N \qquad (1)$$

where M is maximum torque required to tighten the screw, k is material constant and d is nominal diameter of the bolt thread.

In the next step, we analysed the maximum deformations and stresses.

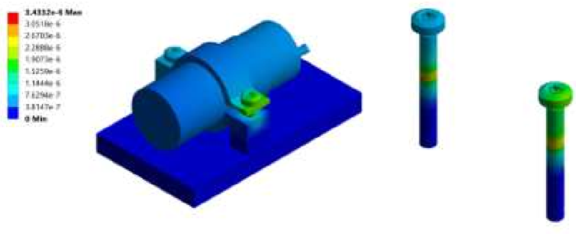

Figure 3 Total deformation of the assembly

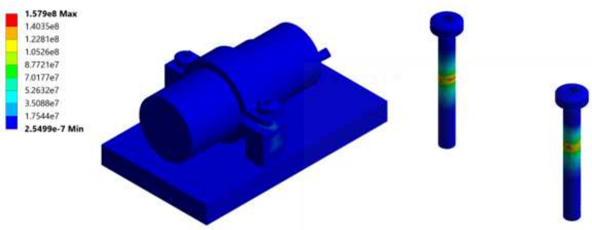

Figure 4 Von Misses stresses of the assembly

Acta Mechatronica - International Scientific Journal about Mechatronics
Volume: 5 2020 Issue: 3 Pages: 35-40 ISSN 2453-7306

The largest deformations occur at the outer face of the bolts, where they reach a value of 0.0034 mm (Figure 3). The stress concentration occurs at the outer face of the bolts where they reach a value 157,9 MPa (Figure 4).

Static analysis provided required data for further modal analysis [4].

5 Dynamic analysis

5.1 *Modal analysis*

This analysis is one of the most widely used types of dynamic analysis. According to the author [5], we can characterize it as a part of dynamics, which defines modal parameters and dynamic behaviour of structures.

If we assume the linear behaviour of the material, then the basic equation of motion of the dynamic analysis will be in the form of a system of linear differential equations of the second order in the matrix form (2):

$$[M]\{\ddot{u}\} + [C]\{\dot{u}\} + [K]\{u\} = \{F\} \quad (2)$$

In the case of modal analysis, we neglect both external load and viscous attenuation, so we can write equation (2) in the form (3) [6]:

$$[M]\{\ddot{u}\} + [K]\{u\} = 0 \qquad (3)$$

The results of the modal analysis in the form of mode shapes with the corresponding natural frequency for the original structural steel model are in Table 2.

Comparison of the natural frequencies results for all three applied materials are shown in Figure 5.

Table 2 Results of modal analysis

	ω (Hz)	Mode shape		ω (Hz)	Mode shape
1.	1701	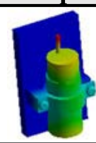	2.	3905	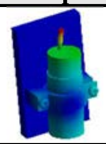
3.	4520,7	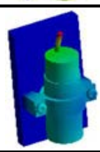	4.	4820,4	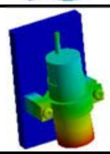
5.	6367	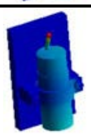	6.	7606,5	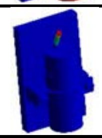

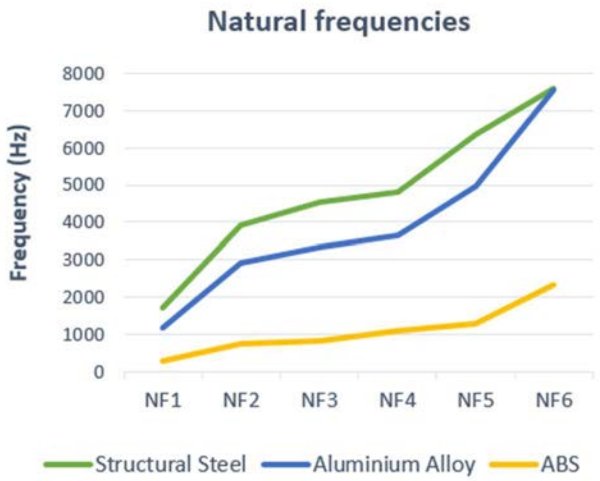

Figure 5 Natural frequencies of the assembly

The performed modal analysis determined the first six mode shapes with corresponding natural frequencies. These first six modes are enough to perform further analyses as it provides input information for both the random vibration testing and the shock testing [7-20].

5.2 *Random vibration testing*

To simulate the tests, linear dynamic calculations were performed in a predefined frequency range [2].

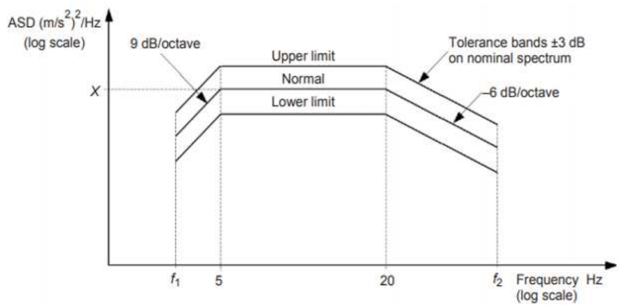

		Direction		
		X	Y	Z
Category 1B	Functional test ASD level (m/s²)²/Hz	0,0060	0,0144	0,0301
	Effective value m/s²	0,45	0,70	1,01
Category 2	Functional test ASD level (m/s²)²/Hz	0,144	0,0414	0,190
	Effective value m/s²	4,70	2,50	5,40

Figure 6 Parameters of random vibration testing [2]

This range was used to obtain vibration responses caused by random vibration excitation. This excitation was defined by accelerated power spectral density (ASD) curves with the prescribed frequency range and root mean square spectrum values given in the standard [2].

All values used in excitation process with the corresponding course of the graph are shown in the Figure 6.

5.2.1 Results

The result of the random vibration tests for Category 1B (Table 3) and Category 2 (Table 4) are the RMS von Mises fields with the specific values given in the tables.

Table 3 Random vibration testing: Results for category 1B

Direction	Structural Steel 13 240	Aluminium Alloy 6061	Plastic ABS
X_norm. (MPa)	0.0053682	0.0052499	0.034317
X_incr. (MPa)	0.009758	0.0061394	0.051746
Y_norm. (MPa)	0.0095404	0.0095111	0.025356
Y_incr. (MPa)	0.015117	0.013135	0.080164
Z_norm. (MPa)	0.021856	0.018751	0.1159

Table 4 Random vibration testing: Results for category 2

Direction	Structural Steel 13 240	Aluminium Alloy 6061	Plastic ABS
X_norm. (MPa)	0.055436	0.054317	0.35735
X_incr. (MPa)	0.10098	0.063717	0.58978
Y_norm. (MPa)	0.034331	0.034	0.090949
Y_incr.. (MPa)	0.053884	0.046807	0.31477
Z_norm. (MPa)	0.11617	0.073302	0.67856

The results are given for the X direction, the Y direction and the Z direction. The highest effective excitation value occurring in the vertical Z direction. This value is then also used for the transverse direction X and the longitudinal direction Y as an increased excitation level [2].

The comparison of the results of the maximum reduced stress values for all three materials and for each direction are shown in Figure 7 for Category 1B and in Figure 8 for Category 2, evaluating the state where the value of maximum reduced stresses is greater than the yield strength of the material used.

Such a condition is considered unsatisfactory because undesired deformations are expected.

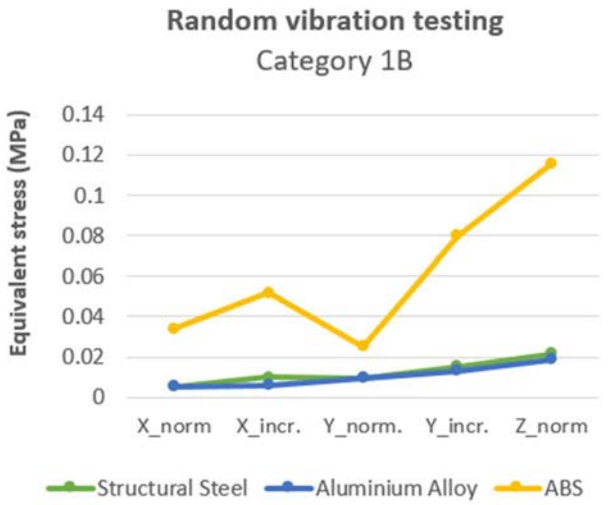

Figure 7 Random vibration testing: Comparison of the results for Category 1B

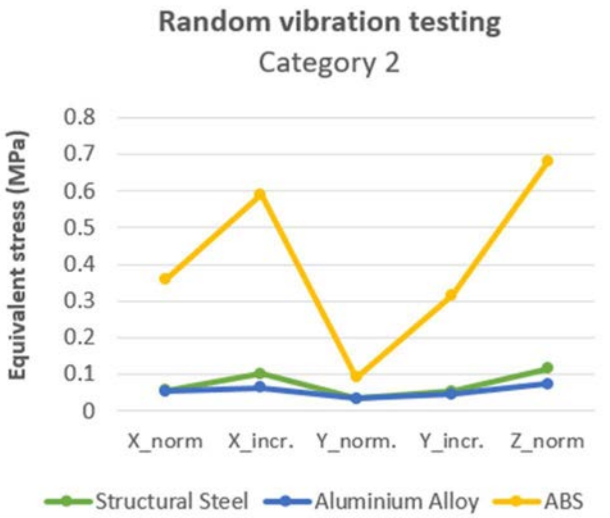

Figure 8 Random vibration testing: Comparison of the results for Category 2

It is clear from the results that the yield strength was not exceeded in any direction of stress for individual materials, so we can say that the item under test conformed with the performance tests after the vibration testing identified in standard [2].

5.3 Shock testing

To simulate the tests, linear dynamic calculations were performed in a predefined time domain, which were used to obtain vibration responses during shock excitation. This excitation was defined by acceleration time courses using three positive and three negative pulses and the time required for the responses to subside. It was also necessary to define the amplitude and width of the pulses (Figure 9).

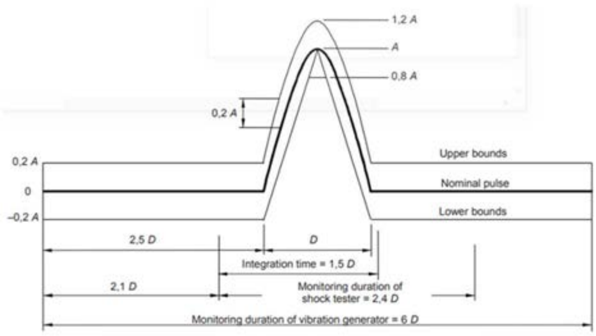

		Direction		
		X	Y	Z
Category 1B	Peak acceleration (m/s²)	30	50	30
	Nominal duration (ms)	30	30	30
Category 2	Peak acceleration (m/s²)	300	300	300
	Nominal duration (ms)	18	18	18

Figure 9 Parameters of shock testing [2]

5.3.1 Results

The result of the shock tests for Category 1B (Table 5) and Category 2 (Table 6) are the RMS von Mises fields with the specific values given in the tables.

Table 5 Shock testing: Results for category 1B

Direction	***Structural Steel 13 240***	***Aluminium Alloy 6061***	***Plastic ABS***
X_norm. (MPa)	0.0005067	0.0006767	0.020885
X_incr. (MPa)	0.0008445	0.0011279	0.034808
Y_norm. (MPa)	0.0011277	0.0014311	0.086949
Z_norm. (MPa)	0.0036982	0.003909	0.19823
Z_incr. (MPa)	0.0061636	0.006515	0.33038

Table 6 Shock testing: Results for category 2

Direction	***Structural Steel 13 240***	***Aluminium Alloy 6061***	***Plastic ABS***
X_norm. (MPa)	0.0064913	0.00883	0.68591
Y_norm. (MPa)	0.010594	0.019368	0.4245
Z_norm. (MPa)	0.060216	0.10024	2.6137

The results are given for the X direction, the Y direction and the Z direction, with the highest excitation effective value occurring in category 1B in the longitudinal direction Y. This value is then also used for the transverse direction X and the vertical direction Z as an increased excitation level. For category 2, the effective excitation values are the same in all directions [2].

The results of the maximum reduced stress values for all three materials and for each direction are shown in Figure 10 for Category 1B and in Figure 11 for Category 2, evaluating the state where the value of maximum reduced stresses is greater than the yield strength of the material used. Such a condition is considered unsatisfactory because undesired plastic deformations are expected.

Figure 10 Shock testing: Comparison of the results for Category 1B

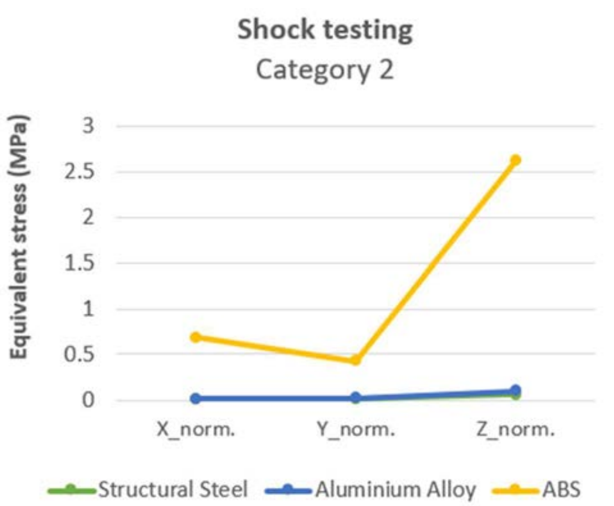

Figure 11 Shock testing: Comparison of the results for Category 2

It is clear from the results that the yield strength was not exceeded in any direction of stress for individual materials, so we can say that the item under test conformed with the performance tests after the vibration testing identified in standard [2].

6 Conclusion

The topic of this article was the dynamic analysis of the sensor OsiSense XS mounting bracket in accordance with the standard EN 61373: 2010.

The aim of the analysis was to assess the suitability of the bracket design. In developing this issue, theoretical knowledge about the finite element method and the subsequent use of the optimization process to improve the final design of the solution were used.

By evaluating the results of the maximum reduced stresses obtained in the random vibration tests as well as in the shock tests, it is obvious that neither material has reached its yield strength. Therefore, all three material designs meet the standard. However, in terms of weight and economic aspect, the best design is the mounting bracket model made of ABS Plastic, which, despite its low specific weight, is an extremely durable material and therefore met all testing parameters [3-20].

Acknowledgement

This article was funded by Ministry of Education of Slovakia Foundation, grant project VEGA no. 1/0290/18 and KEGA 027TUKE-4/2020.

References

[1] BATHE, K.J.: *Finite Element Procedures in Engineering Analysis*, New Jersey: Prentice Hall, Inc. Englewood Cliffs, 1982.

[2] BS EN 61373:2010, *Railway applications — Rolling stock equipment — Shock and vibration tests*, The British Standards Institute, 2010.

[3] DAHALE, P., PAWAR, P.: Assessment of boundary conditions for FEA of mounting bracket using co-relation with experimental results, *Measurement*, Vol. 12, No. 3, pp. 141-143, 2018.

[4] KIRTHANA, S., NIZAMUDIN, N.: Finite element method analysis and topology optimization of engine mounting bracket, *Mechanical Structures*, Vol. 13, No. 4, pp. 123-125, 2018.

[5] KRISHNA, G., TARAK, D., BURMAN, R.: Numerical and experimental comparative study of Aluminium and hybrid mounting interfaces of launch vehicle avionics for weight reduction, *Procedia Structural Integrity*, Vol. 14, pp. 820-829, 2019.

[6] TAVARES, S., PARDAL, J.: Failure during fabrication of clamps of Mn-alloyed steel for springs in heavy vehicles, *Engineering Failure Analysis*, Vol. 109, No. 4, pp. 112-120, 2020.

[7] BOERMA, J.R., KALS, S.R.: Fixture Design with FIXES: The Automatic Selection of Positioning, Clamping and Support Features for Prismatic Parts, *CIRP Annals*, Vol. 38, No. 1, pp. 399-402, 1989.

[8] WANG, Z.: Clamp looseness detection using modal strain estimated from FBG based operational modal analysis, *Measurement*, Vol. 137, No. 1, pp. 82-97, 2019.

[9] SONG, B., WANG, H.: Dynamic simulation and optimization of clamping mechanism of online tension testing machine for wire ropes, *Engineering Failure Analysis*, Vol. 95, No. 5, pp. 181-190, 2019.

[10] WANG, Y., LIU, S.: A method of railway system safety analysis based on cusp catastrophe model, *Accident Analysis & Prevention*, Vol. 151, No. 13, pp. 51-64, 2021.

[11] LI, Z., ZHANG, C.: Design and parameter optimization of contactless vertical inductive angle sensor, *Vacuum*, Vol. 169, No. 23, pp. 141-156, 2019.

[12] VO, D., BORKOVIC, A.: Dynamic multi-patch isogeometric analysis of planar Euler–Bernoulli beams, *Computer Methods in Applied Mechanics and Engineering*, Vol. 372, No. 3, pp. 41-46, 2020.

[13] ZHANG, H., ZHU, X.: Nonlinear dynamic analysis method for large-scale single-layer lattice domes with uncertain-but-bounded parameters, *Engineering structures*, Vol. 203, No. 5, pp. 12-19, 2020.

[14] THAKUR, B.: Geometrically nonlinear dynamic analysis of laminated composite plate using a nonpolynomial shear deformation theory, *International Journal of Non-Linear Mechanics*, Vol. 128, No. 15, pp. 192-198, 2021.

[15] MALÁKOVÁ, S., FRANKOVSKÝ, P., NEUMANN, V., KURYLO, P.: Evaluation of suppliers' quality and significance by methods based on weighted order, *Acta logistica*, Vol. 7, No. 1, pp. 1-7, 2020.

[16] LIU, G.R., QUEK, S.S.: *Finite Element Method: A Practical Course*, Butterworth-Heinemann, 2003.

[17] LIANG, J.: *A user-defined element for dynamic analysis of saturated porous media in ABAQUS*, Computers and Geotechnics, 2020.

[18] SERHAT, G., BEDIZ, B.: Dynamic analysis of doubly curved composite panels using lamination parameters and spectral-Chebyshev method, *Mechanical Structures*, Vol. 126, No. 10, pp. 169-174, 2020.

[19] RAHNAVARD, R., NAPOLITANO, R.: Static and dynamic stability analysis of a steel-rubber isolator with rubber cores, *Computers & Structures*, Vol. 26, No. 10, pp. 441-455, 2020.

[20] HU, Y., WANG, X.: Dynamic analysis of offshore steel wind turbine towers subjected to wind, wave and current loading during construction, *Ocean Engineering*, Vol. 216, No. 20, pp. 231-236, 2020.

Acta Mechatronica - International Scientific Journal about Mechatronics
Volume: 5 2020 Issue: 3 Pages: 41-46 ISSN 2453-7306

doi:10.22306/am.v5i3.67

Received: 02 July 2020
Revised: 24 July 2020
Accepted: 15 Aug. 2020

COMPUTER SIMULATION USING MSC ADAMS

Darina Hroncová
Department of Mechatronics, Faculty of Mechanical Engineering, Technical University of Košice, Park Komenského 8, 042 00 Košice, Slovakia, EU, darina.hroncova@tuke.sk
Ingrid Delyová
Department of Mechatronics, Faculty of Mechanical Engineering, Technical University of Košice, Park Komenského 8, 042 00 Košice, Slovakia, EU, ingrid.delyova@tuke.sk

Keywords: **s**imulation, two-link manipulator, kinematic analysis, controller

Abstract: The goal of the presented paper is to compile a two-link model of manipulator and control the movement of the basket mounted at its end-effector. Authors focus on using MSC Adams in simulation of the motion of a two-link manipulator model. Attention is paid to kinematic and dynamic analysis of the manipulator, its modelling and control. The capability of MSC Adams Control Toolkit is used to design a control system which keeps the basket of the end-effector in horizontal position. Finally, the results obtained by computer simulation of the model are evaluated.

1 Introduction

A significant advantage of computer simulation of prototype models is the ability to immediately visualize modifications of design variants as well as the consequences of these changes on the behavior of the entire system.

Computer simulation allows to create a virtual prototype of a device and adjust it or create new variants of it without actually producing the real device. The change of behavior of these different variants of the model can be studied. By simulation we can also display the proposed model in its work cycle thus revealing possible collisions of its elements and evaluate different parameters of interest and visualize them in the software. The operation of the model can understood and subsequently verified its efficiency. During the simulation the values of different parameters can be checked in respective output displays of the simulated model in real time [1,3-7].

2 Model of manipulator

The aim of the paper is to analyse the compiled model of a two link manipulator shown in the figure (Figure 1). From the kinematic point of view the manipulator structure is represented by an open kinematic chain [2-8].

The manipulator consists of two arms mounted on a solid base. The base ensures the manipulator stability in operation. The working tool, which in our case is a basket, is firmly attached to the end-effector of the manipulator. The manipulator then performs a working cycle with the basket. Our goal is to describe the motion of the end-effector. The next chapters describe the kinematic analysis of the motion of the end-effector [2-8,22].

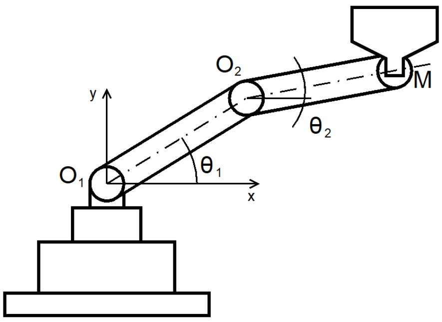

Figure 1 Model of the two link manipulator

The next figure (Figure 2) shows the model of a two link manipulator created in MSC Adams [8,22]. It consists of two links of length l_1 and l_2, with weights m_1 and m_2. We consider two degrees of freedom of movement. The arms are connected by rotating kinematic pairs to each other and by another rotating kinematic pair to the base. The drives are placed in respective kinematic pairs. The angle of rotation in kinematic pairs is denoted by angles θ_1 and θ_2. Kinematic equations describing the position of the end point M of the manipulator (Figure 2) depending on the angles of rotation θ_1 and θ_2 are expressed as follows [2].

$$x_M = l_1 \cos\theta_1 + l_2 \cos(\theta_1 + \theta_2) \tag{1}$$

$$y_M = l_1 \sin\theta_1 + l_2 \sin(\theta_1 + \theta_2) \tag{2}$$

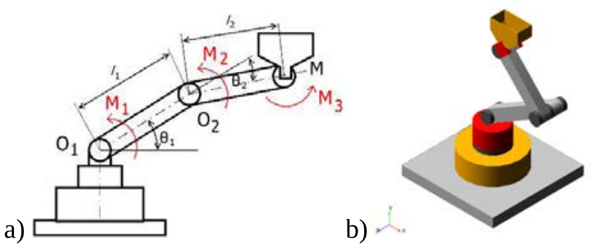

Figure 2 a) Model of the two link manipulator, b) model of the two link manipulator in MSC Adams/View

The driving torques M_1 and M_2 are triggered by servo drives in individual kinematic pairs. They ensure the movement of the manipulator arms. The notation of dynamic equations of motion of the manipulator (Figure 1) can be briefly written according to [3-8]:

$$M(\theta)\ddot{\theta}+V(\theta,\dot{\theta})+G(\theta)=\tau \tag{3}$$

where $M(\theta)$ is the inertia matrix, $V(\theta,\dot{\theta})$ is the Coriolis-centripetal vector, G(θ) is the gravity vector and τ is vector of actuator torques.

Equation (3) in our case represents a model with 2° of freedom of motion, a system of two 2nd order differential equations. The motion of the mechanism of the two link manipulator takes place in vertical plane, for this reason the influence of gravity is also taken into account. The equations of motion do not take into account the laxity and friction effects in the individual kinematic pairs nor the elastic deformations of the individual arms of the manipulator [9-13]. We consider the change of the weight of the basket due to the load of material present in the basket [22].

3 Computer simulation

A 3D computer model of a two link manipulator is created in MSC Adams. Modelling elements and procedures for the creation of bodies and their kinematic bonds were used. After proposing the model, the functionality is verified and the simulation is started Figure 3 [1,3-8,22].

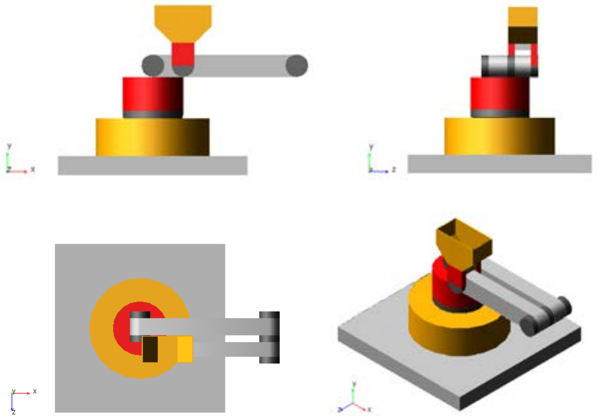

Figure 3 Views of the rendered model

Figure 4 shows the simulation of the model with the compensating torque [9-14].

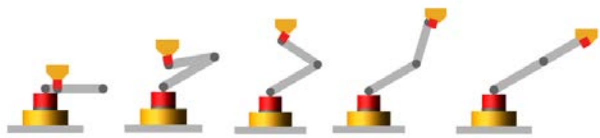

Figure 4 Views of the rendered model

Next we focus on controlling the position of the basket during the motion. The basket can be used for manipulation of materials of various kinds, namely solid, bulk or liquid. The control was performed in MSC Adams. It offers the possibility of creating a control system using different types of controllers. In our case, we use a proportional controller with gain K_p.

The compensating torque in Figure 5 is needed to control the current position of the basket with respect to the desired position during motion. The SFORCE_1 torque secures the position of the basket in a horizontal position and thus prevents the loss of stability during the motion.

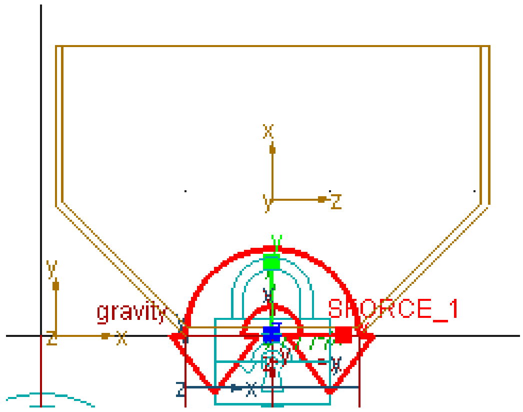

Figure 5 Compensating Torque SFORCE_1

The stability of the basket is ensured with a control circuit by means of a balancing torque which stabilizes the basket during the motion. A feedback control circuit is provided, i.e. a torque controller to keep the basket in horizontal position during the motion of the arm [22]. There is a diagram of a closed feedback basket position control system with a proportional controller K_p in the next picture (Figure 6) [14-22].

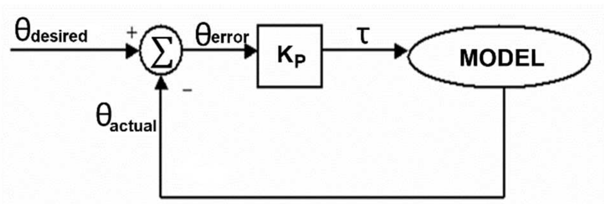

Figure 6 The control system with proportional feedback

The control system ensures that the compensating torque keeps the end-effector in horizontal position and the loss of stability of the basket during the motion of the manipulator is prevented. The control circuit of the system is designed according to the diagrams in Figure 6 and Figure 7.

Volume: 5 2020 Issue: 3 Pages: 41-46 ISSN 2453-7306

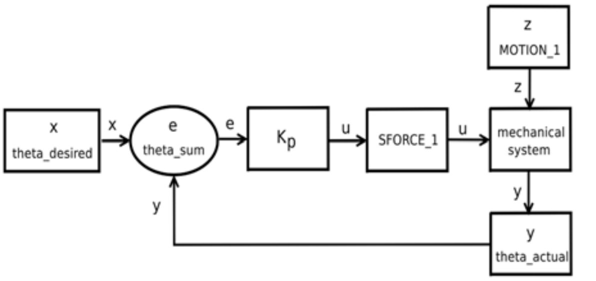

Figure 7 Scheme of control system with proportional controller

The mechanical system is controlled by the variable u according to the following equation:

$$u=K_p.e \tag{4}$$

where in the diagram in Figure 7:

- u – torque control action variable (torque_gain) for compensating torque (SFORCE_1),
- x – desired angle (theta_desired = 0°),
- y – measured controlled variable (theta_actual),
- e – difference (error) in the adding block: theta_sum = theta_desired - theta_actual,
- z – fault quantity (prescribed movement of the mechanical system).

After compiling the block diagram of the control system we need to define the following elements:

- Design Variable
- State Variable
- Measure

We define the control system in MSC Adams using the Controls Toolkit. Its control blocks menu is shown in Figure 8 [22].

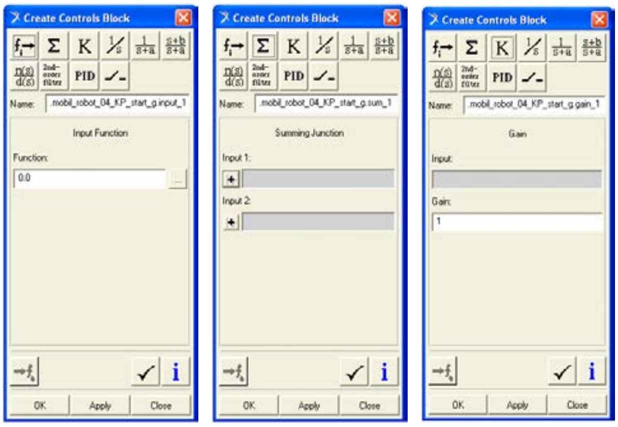

Figure 8 Controls Toolkit – Create Controls Block

The first input signal to the summation block is the desired value of the angle ($\theta_{desired}$) between the x axis defined on the end-effector and the axis of the base reference system, which is zero. In the Create Control Blocks dialog box (Figure 7) we select the input signal f_i and define the desired input variable (*theta_desired*). We set the required value of the angle to 0°.

The control difference between the desired and the actual angle is defined in the *summing junction block* (∑). Subtracting the current angle value from the desired angle of the basket during the motion is *theta_error* and is written to the *Database Navigator.*

The gain block provides the u signal amplification for control of the basket position compensation torque (SFORCE_1). The input for the gain block is *theta_error* variable created in the previous section. After setting the amount of gain and its input, an element (*torque_gain*) is added to the *Database Navigator* (Figure 9).

After assigning the created function the variables are written and displayed in the *Database Navigator*. The content of the variables is in (Figure 9):

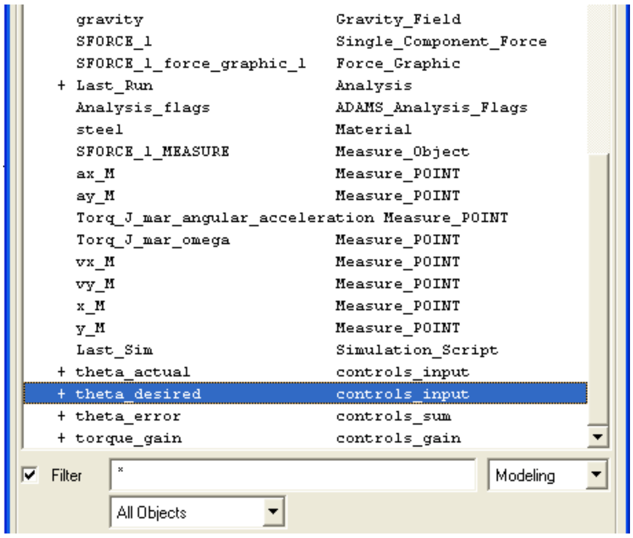

Figure 9 Database Navigator of the model of manipulator

Interactive simulation and visualization allows comfortable simulation of the model, model modifications and visualization of results. The graphs of output variables enable viewing the current values of the measured variables in real time during the actual simulation and its visualization (Figure 10).

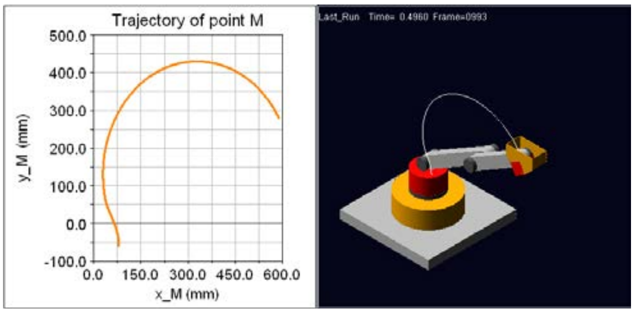

Figure 10 The animation of the simulation and displacement of the end-effector

It is also possible to display the model in the current state and print the results prepared this way (Figure 10). Postprocessor is an integral part of the process of computer modeling of a prototype and it is a very comfortable tool for creating, processing, modifying and presenting the results of simulation in the form of graphs [8-14]. It is also possible to create the output of the simulation in AVI format.

4 Resulting kinematic parameters

The values of the calculated variables are displayed in a graphical form with the postprocessor. The magnitudes of the torques in rotating kinematic pairs when the weights of the arms are $m_1 = 9.9779$ kg, $m_2 = 7.1330$ kg and the weight of the basket $m_b = 0.9348$ kg are in Figure 11 to Figure 13.

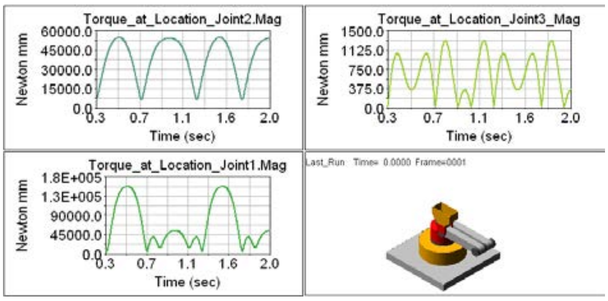

Figure 11 The graph of the torque in the joint 1, joint 2 and joint 3

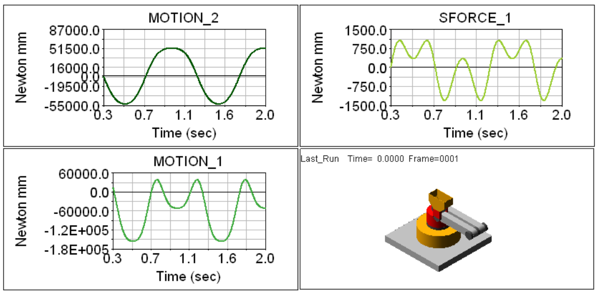

Figure 12 The graph of the torque MOTION_1, MOTION_2 and SFORCE_1

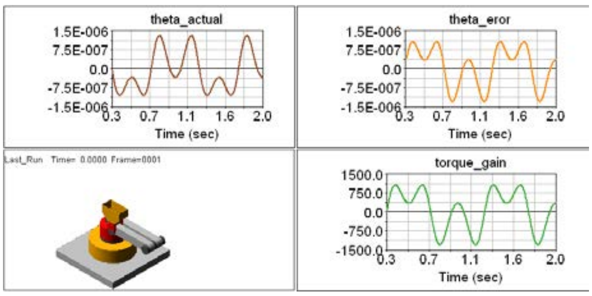

Figure 13 The graph of the angle theta actual, theta error and theta desired

The magnitudes of the moments in rotating kinematic pairs with increased arm and weight of the basket $m_b = 0.9$ kg, $m_b = 5$ kg and $m_b = 10$ kg are calculated next. The magnitude of the moments in joints are shown in Table 1, Table 2 and Table 3.

Table 1 The magnitude of the MOTION_1

MOTION_1 (N·mm)		
	t=0.222 (sec)	**t=0.5 (sec)**
m_b=0.9 (kg)	838288.775	-156420.0
m_b=5.0 (kg)	84295.6345	-234500.0
m_b=10.0 (kg)	141230.0	-330530.0

Table 2 The magnitude of the MOTION_2

MOTION_2 (N·mm)		
	t=0.5 (sec)	**t=1.0 (sec)**
m_b=0.9 (kg)	-52659.4247	51970.7031
m_b=5.0 (kg)	-88877.8319	85194.0907
m_b=10.0 (kg)	-133420.0	126050.0

Table 3 The magnitude of the SFORCE_1

SFORCE_1 (N·mm)		
	t=0.638 (sec)	**t=0.818 (sec)**
m_b=0.9 (kg)	1060.8687	-1307.8291
m_b=5.0 (kg)	5677.3421	-6999.5562
m_b=10.0 (kg)	11354.7405	-13999.1839

Before starting the simulation a change of the magnitudes of individual moments in individual joints is expected, as well as change of the compensating moment of the end-effector [16,17]. The graphs obtained by the simulation are shown in (Figure 14 - 16). Only the torques are plotted. Angular variables as acceleration, speed and trajectories are not changed by the load. The resulting graphs are in the following figures.

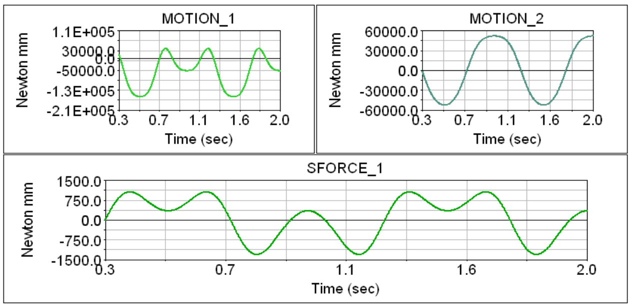

Figure 14 The graphs of the torques in the joints with weight of the basket m_b=0.9kg

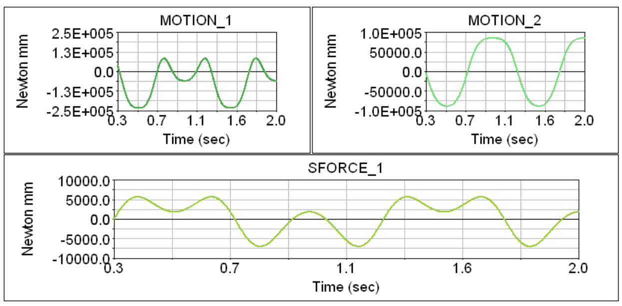

Figure 15 The graphs of the torques in the joints with weight of the basket m_b=5kg

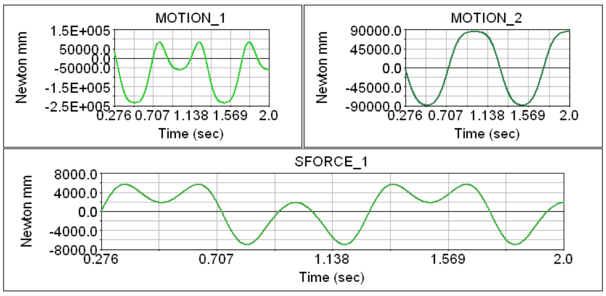

Figure 16 The graphs of the torques in the joints with weight of the basket m_b=10kg

We also calculated the values of position, velocity and acceleration of the basket (Figure 17 - 19) [20].

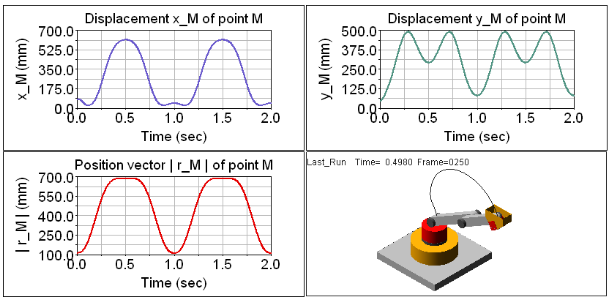

Figure 17 The graph of the position x_M and y_M of the end-effector

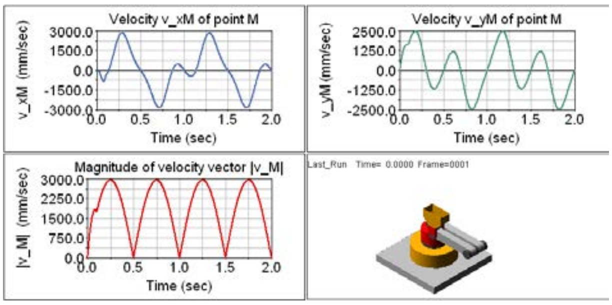

Figure 18 The graph of the velocity v_{xM} and v_{yM} of the end-effector

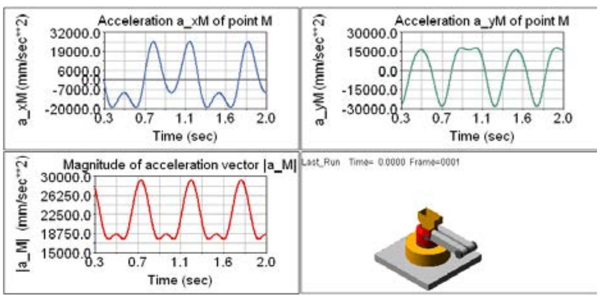

Figure 19 The graph of the acceleration a_{xM} and a_{yM} of the end-effector

The aim was also to obtain results from the control of the end-effector and prove the ability and functionality of the proposed regulator for the compensating torque. The obtained graphs of the actual and desired angle during the motion along the trajectory are shown in Figure 13. The difference between these values is in negligible ranges in both cases which indicates a suitably designed and functional end-effector position control system [20-22].

Conclusions

The values obtained from both simulations confirmed the increase and decrease of the acting torques in the joints of the manipulator. An increase in the load also revealed an increase in the torque required to move the basket along the trajectory. The opposite is true when reducing the load.

MSC Adams works with a 3D model [22]. The advantage is the possibility to simulate the motion of the prototype model and its control in the program environment and verification of the functionality in the form of 3D visualization. Based on the results obtained from the simulation it is possible to build a real model and design the drives. When designing drives for a mechanical system it is necessary to pay attention to the maximum magnitudes of the forces when handling various loads and so it is necessary to design the drive with the appropriate parameters for the specific purpose of use of the manipulator.

The proposed control of the stability of the end-effector by selecting the appropriate control system and setting the controller parameters is an important aspect for maintaining stability and managing load transfer. Based on the results of the simulation it can be stated that the proposed control system is functional and maintains the necessary stability during the motion of the manipulator. Simulation software is a suitable tool for design, saving time and resources. It is also suitable for detailed research and investigation of mechanical systems in practice.

Acknowledgement

The authors would like to thank to Slovak Grant Agency project VEGA 1/0389/18 and VEGA 1/0290/18, grant projects KEGA 018 TUKE-4/2018 and grant projects KEGA 030 TUKE-4/2020 supported by the Ministry of education of Slovak Republic.

References

[1] HRONCOVÁ, D., DELYOVÁ, I., FRANKOVSKÝ, P.: Kinematic Analysis of Mechanism Using MSC Adams, *Applied Mechanics and Materials*, Vol. 611, No. 7, pp. 83-89, 2014.

[2] BAKŠI, J.: *Control of a two-link 2-DOF robot manipulator with variable load*, Diploma thesis, Technical university of Kosice, Faculty of Mechanical Engineering, Department of Mechatronics, Slovakia, 2017. (Original in Slovak)

[3] DELYOVÁ, I., HRONCOVÁ, D., FRANKOVSKÝ, P.: Analysis of Simple Mechanism Using MSC Adams, *Manufacturing Technology*, Vol. 14, No. 2, pp. 141-145, 2014.

[4] DELYOVÁ, I., HRONCOVÁ, D., FRANKOVSKÝ, P.: *Kinematic analysis of movement of a point of a*

simple mechanism, 4th International Conference Modelling of mechanical and mechatronics systems, Košice: KAMaM, Technical University Košice, Herľany, Slovakia, 2011.

[5] ŠARGA, P., HRONCOVÁ, D., RÁKAY, R.: The MSC Adams View and Simulation of Crank Rocker Mechanism, *American Journal of Mechanical Engineering*, Vol. 3, No. 6, pp. 161-164, 2015.

[6] HRONCOVÁ, D., RÁKAY, R., LIPTÁK, T.: Sim Mechanics and Forward and Inverse Problem of Dynamics, *Journal of Automation and Control*, Vol. 3, No. 3, pp. 58-61, 2015.

[7] HRONCOVÁ, D., FRANKOVSKÝ, P., BETTES, G.: Kinematical Analysis of Crank Slider Mechanism with Graphical Method and by Computer Simulation, *American Journal of Mechanical Engineering*, Vol. 4, No. 7, pp. 329-343, 2016.

[8] VAVRO, J. Jr., VAVRO, J., KOVÁČIKOVÁ, P., BEZDEDOVÁ, R., HÍREŠ, J.: Kinematic and Dynamic Analysis and Distribution of Stress in Items of Planar Mechanisms by Means of the MSC Adams Software, *Manufacturing Technology*, Vol. 17, No. 2, pp. 267-270, 2017.

[9] MIKOVÁ, Ľ., GMITERKO, A., FRANKOVSKÝ, P., HRONCOVÁ, D.: Impact of dynamics of the frame on the performance of the positioning servosystem, *International Journal of Advanced Robotic Systems*, Vol. 13, No. 5, pp. 1-6, 2016.

[10] KELEMENOVÁ, T., FRANKOVSKÝ, P., VIRGALA, I., MIKOVÁ, Ľ., KELEMEN, M.: Machines for inspection of pipes, *Acta Mechatronica*, Vol. 1, No. 1, pp. 1-7, 2016.

[11] HRONCOVÁ, D., GMITERKO, A., LIPTÁK, T., BRUCHÁNEK, M.: Computer Simulation of the Mechanical System with One Degree of Freedom, *Acta Mechatronica*, Vol. 1, No. 4, pp. 13-18, 2019.

[12] VIRGALA, I., MIKOVÁ, Ľ., VARGA, M., KELEMEN, M.: Didactic Model of Controlled Water Tank System, *Acta Mechatronica*, Vol. 4, No. 3, pp. 1-5, 2019.

[13] VIRGALA, I., MIKOVÁ, Ľ., VARGA, M., KELEMEN, M.: Microcontroller for Mechatronic Systems, *Acta Mechatronica*, Vol. 2, No. 3, pp. 7-12, 2017.

[14] VIRGALA, I., MIKOVÁ, Ľ, KELEMEN, M., HRONCOVÁ, D.: Snake Like Robot, *Acta Mechatronica*, Vol. 3 , No. 4, pp. 7-10, 2018.

[15] GMITERKO, A., MIKOVÁ,Ľ., ŠARGA, P., BOBOVSKÝ, Z.: *Control of technical systems*, TU Košice, 2013. (Original in Slovak)

[16] MIKOVÁ, Ľ., GMITERKO, A., KELEMEN, M., VIRGALA, I., PRADA, E., HRONCOVÁ, D., VARGA, M.: Motion control of nonholonomic robots at low speed, *International Journal of Advanced Robotic Systems*, Wien: Technische Universität Wien, Vol. 17, No. 1, pp.1-12.

[17] LIPTÁK, T., KELEMEN, M., GMITERKO, A., VIRGALA, I., HRONCOVÁ, D.: The control of holonomic system, *Acta Mechatronica*, Vol. 1, No. 2, pp. 15-20, 2016.

[18] PIRNÍK, R., HRUBOŠ, M., NEMEC, D., BOŽEK, P.: Navigation of the autonomous ground vehicle utilizing low-cost inertial navigation, *Acta Mechatronica*, Vol. 1, No. 1, pp. 19-23, 2016.

[19] BOŽEK, P., TURYGIN, Y.: Measurement of the operating parameters and numerical analysis of the mechanical subsystem, *Measurement Science Review*, Vol. 14, No. 4, pp. 198-203, 2014.

[20] ABRAMOV, I. V., NIKITIN, Y. R., ABRAMOV, A. I., SOSNOVICH, E. V., BOŽEK, P.: Control and Diagnostic Model of Brushless DC Motor, *Journal of Electrical Engineering*, Vol. 65, No. 5, pp. 277–282, 2014.

[21] JURUŠ, O., SUKOP, M., ŠPAK, M., ŠTOFA, M. Manipulator Arm for Robot SCORPIO, *American Journal of Mechanical Engineering*, Vol. 4, No. 7, pp. 349-352, 2016.

[22] Adams, The Multibody Dynamics Simulation Solution: [Online], Available: http://www.mscsoftware.com/product/adams [20 june 2020], 2020.

JOURNAL STATEMENT

Journal name: **Acta Mechatronica**
Abbreviated key title: Acta Mechatron
Journal title initials: AM
Journal doi: 10.22306/am
ISSN: 2453-7306
Start year: 2016
The first publishing: March 2016
Issue publishing: Quarterly
Publishing form: On-line electronic publishing
Availability of articles: Open Access Journal
Journal license: CC BY-NC
Publication ethics: COPE, ELSEVIER Publishing Ethics
Plagiarism check: Worldwide originality control system
Peer review process: Single-blind review at least two reviewers
Language: English
Journal e-mail: **info@actamechatronica.eu**

The journal focuses mainly on original, interesting, new and quality, theoretical, practical and application-oriented contributions to the scientific fields and research as well as to pedagogy and training in mechatronics.

Publisher: **4S go, s.r.o.**
Address: Semsa 24, 044 21 Semsa, Slovak Republic, EU
Phone: +421 948 366 110
Publisher e-mail: **info@4sgo.eu**

Responsibility for the content of a manuscript rests upon the authors and not upon the editors or the publisher.